Optical coherence gratings and lattices

Liyuan Ma and Sergey A. Ponomarenko*

Department of Electrical and Computer Engineering, Dalhousie University, Halifax, NS B3J 2X4, Canada
**Corresponding author: serpo@dal.ca*

Received October 7, 2014; accepted October 21, 2014;
posted October 24, 2014 (Doc. ID 224490); published November 21, 2014

We introduce a class of partially coherent temporal/spatial sources, optical coherence gratings/lattices that have a Gaussian intensity profile and statistically stationary/homogeneous, periodic temporal/spatial coherence properties. We show that temporal coherence gratings generate partially coherent pulses with periodic spectra, whereas spatial coherence lattices yield far-zone output in the form of periodic lattices of highly directional beams.

OCIS codes: (030.0030) Coherence and statistical optics; (030.1640) Coherence; (030.4070) Modes; (050.1950) Diffraction gratings; (320.5550) Pulses.
http://dx.doi.org/10.1364/OL.39.006656

There has lately been growing interest in designing novel partially coherent optical sources catering to a multitude of applications to optical communications, image transfer, and optical lithography, among others. Until recently, there have been known only a few classes of such sources, either spatial or temporal. Indeed, apart from seminal Gaussian Schell-model sources [1], only a few other classes emerged for which closed-form analytical expressions for their cross-spectral densities or two-time correlation functions can be obtained. Twisted Gaussian Schell-model sources [2], which can be represented viz coherent mode decompositions of either Hermite–Gaussian [3] or Laguerre–Gaussian [4] modes, Bessel-correlated [5], modified-Bessel-correlated sources, generating partially coherent vortex fields [6], as well as dark and antidark diffraction-free sources [7], comprised all such known classes until late. All just mentioned partially coherent sources were either constructed or analyzed theoretically using the classic coherent mode representation of optical coherence theory [1]. Some such sources have also been experimentally realized to date [8,9].

The introduction of a general representation for partially coherent sources, ensuring the generated fields to have bona fide correlation properties, has given new impetus to the field [10]. A multitude of partially coherent spatial and temporal sources were devised using the prescriptions of [10], including Gaussian sources with nonuniform correlations [11], flat-top field generating sources [12], Bessel– and Laguerre–Gaussian [13], circular cosine–Gaussian [14,15], rectangular multi-Gaussian [16], temporal sources with tunable coherence profiles [17], and difference-Gaussian [18] Schell-model sources. In addition, new independent-elementary-source decomposition [19] and complex Gaussian representation (CGR) [20] were introduced. While being particular forms of [10], the novel representations nonetheless open up alternative avenues for partially coherent source design. In particular, the CGR was shown to provide a convenient vehicle to devise trains of partially coherent pulses [20]. Moreover, due to over-completeness of the CGR modes, any partially coherent source has a CGR as was shown in [20]. Yet, the CGR power for new partially coherent source synthesis has barely been explored to date.

In this work, we employ the CGR to construct wide classes of temporal and spatial partially coherent sources that we term optical coherence gratings and lattices. All novel sources generate either statistically stationary pulses or statistically homogenous beams with Gaussian intensity profiles in the source plane. Thus, they are all of a Schell-model type. Yet, their coherence properties are periodic in time or space, and hence the name optical coherence gratings or lattices. In the temporal case, novel sources generate periodic trains of quasi-monochromatic components. In the spatial case, the novel sources give rise to periodic arrays of highly directional beams in the far zone of the source. The discovered sources can find applications to optical imaging with partially coherent light, optical information transfer through natural environments, where partially coherent pulses/beams are more robust in presence of media fluctuations and to optical lithography, to name but a few.

Temporal coherence gratings: According to the CGR, a two-time correlation function of any partially coherent source can be represented as [20]:

$$\Gamma(T_1, T_2) = \int \mathrm{d}^2\alpha\, \mathcal{P}(\alpha)\psi_\alpha^*(T_1)\psi_\alpha(T_2), \tag{1}$$

where $\alpha = \mathrm{Re}\,\alpha + i\,\mathrm{Im}\,\alpha$ is a complex variable; $d^2\alpha \equiv \mathrm{Re}\,\alpha\,\mathrm{Im}\,\alpha$, $\mathcal{P}(\alpha)$ is a nonnegative function to guarantee nonnegative definiteness of Γ [1,10,20]. Hereafter, we will use dimensionless time and frequency variables, $T = t/\tau_\mathrm{p}$ and $\Omega = \omega\tau_\mathrm{p}$, where τ_p is a temporal width of the pulse, and assume any time variables to be scaled to τ_p. In the dimensionless variables, complex Gaussian modes,

$$\psi_\alpha(T) = \frac{e^{-(\mathrm{Im}\,\alpha)^2}}{\pi^{1/4}} \exp\left[-\frac{\left(T - \sqrt{2}\alpha\right)^2}{2}\right], \tag{2}$$

form an overcomplete, complete but nonorthogonal, set such that

$$\int \mathrm{d}^2\alpha\, \psi_\alpha^*(T_1)\psi_\alpha(T_2) = \delta(T_1 - T_2). \tag{3}$$

As was discussed in detail elsewhere [20], the complex variable α incorporates time delays and frequency shifts of constituting Gaussian pulses.

Let us restrict ourselves to source classes for which the distribution function $\mathcal{P}$ has the form

$$\mathcal{P}(\alpha) = \sum_n \nu_n \delta(\alpha - \alpha_n), \qquad \nu_n \geq 0. \tag{4}$$

It then follows from Eqs. (1) and (4) that

$$\Gamma(T_1, T_2) = \sum_n \nu_n \psi^*_{\alpha_n}(T_1)\psi_{\alpha_n}(T_2). \tag{5}$$

We note that Eq. (5) is in the form of pseudo-mode expansion discussed in [21], and ν_n characterizes energy distribution among the pseudo-modes.

A particularly interesting family of partially coherent Schell-model sources arises with the choice

$$\alpha_n = i \operatorname{Im} \alpha_n = i \frac{\pi n}{a\sqrt{2}}, \tag{6}$$

implying that there is no time delay, but consecutive Gaussian modes have equal relative frequency shifts. It follows from Eqs. (2), (5), and (6), after elementary algebra, that each such source has a Gaussian intensity,

$$I(T) \equiv \Gamma(T, T) = I_0 e^{-T^2}; \qquad I_0 = \frac{1}{\sqrt{\pi}} \sum_n \nu_n, \tag{7}$$

and its temporal degree of coherence, defined as [1]

$$\gamma(T_1, T_2) \equiv \frac{\Gamma(T_1, T_2)}{\sqrt{I(T_1) I(T_2)}}, \tag{8}$$

can be expressed as

$$\gamma(T_1, T_2) = \frac{\sum_n \nu_n \exp\left[i \frac{\pi n}{a}(T_2 - T_1)\right]}{\sum_n \nu_n}. \tag{9}$$

We can infer from Eq. (9) that (i) discovered optical coherence gratings are statistically stationary and (ii) their coherence properties are time-periodic with a characteristic period of a (in scaled variables).

The energy spectrum, defined as [22]

$$S(\Omega) = \int_{-\infty}^{+\infty} dT_1 \int_{-\infty}^{+\infty} dT_2 \, \Gamma(T_1, T_2) e^{i\Omega(T_1 - T_2)}, \tag{10}$$

reveals energy distribution among monochromatic components of the source. It follows from Eqs. (8)–(10) after straightforward algebra that up to an immaterial factor, energy spectra of novel sources are given by

$$S(\Omega) \propto \sum_n \nu_n e^{-(\Omega - \pi n/a)^2}. \tag{11}$$

It is a periodic Gaussian frequency comb with distinct quasi-monochromatic components that fail to overlap for a sufficiently small period a of the coherence grating.

Quantitative features of discovered coherence gratings and resulting statistical frequency combs depend on the mode energy distribution ν_n. Consider, for instance, a grating of finite number N of equally weighted complex Gaussians with $\nu_n = \nu = \text{const}$. Such a distribution yields a closed-from expression for γ such that

$$|\gamma(T_1, T_2)| = \left| \frac{\sin\left[\frac{\pi N}{2a}(T_2 - T_1)\right]}{N \sin\left[\frac{\pi}{2a}(T_2 - T_1)\right]} \right|, \tag{12}$$

which is displayed in Fig. 1 for two values of N. For large enough N, Eq. (12) is reminiscent of a classic pattern generated by illuminating a diffraction grating with a coherent plane wave in the far zone of the grating [23]. A quick glance at Fig. 1(b) confirms the conclusion. The corresponding energy spectrum is exhibited in Fig. 2. It is clearly seen in the figure that the spectrum represents a periodic train of quasi-monochromatic components, provided the number of coherence grating lobes is sufficiently large, $N \gg 1$, and their period sufficiently small, $a < 1$.

Another instructive example is furnished by an infinite number of CGs weighted according to $\nu_n = \lambda^n/n!$ where $\lambda > 0$ is a free parameter. The corresponding temporal degree of coherence sums to

$$|\gamma(T_1, T_2)| = \exp\left\{-2\lambda \sin^2\left[\frac{\pi(T_2 - T_1)}{2a}\right]\right\}. \tag{13}$$

We show the temporal degree of coherence and energy spectrum in Fig. 3. It is seen in the figure that this source possesses diffraction grating-like coherence properties resulting in a periodic energy spectrum as well. Unlike the case in Fig. 2, however, the spectral train is amplitude modulated here. Owning to qualitative agreement between the two cases, we can conclude that the whole class of sources, specified by (9), gives rise to optical coherence gratings.

Spatial coherence lattices: A 2D generalization of the above describes spatial sources producing random beams. In the space-frequency representation, we seek the cross-spectral density of a beam field ensemble at a pair of points $\boldsymbol{\rho}_1$ and $\boldsymbol{\rho}_2$ in the source plane in a factorized form

$$W(\boldsymbol{\rho}_1, \boldsymbol{\rho}_2) = \prod_{s=X,Y} W(s_1, s_2). \tag{14}$$

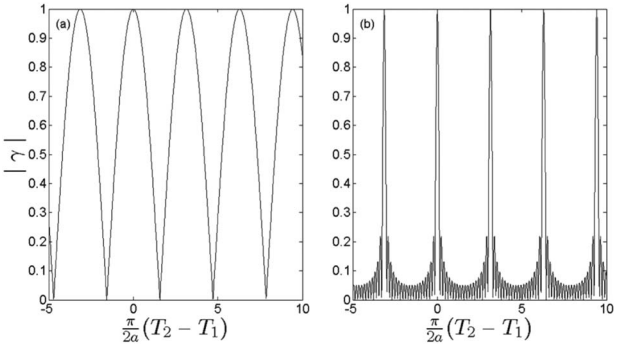

Fig. 1. Modulus of the temporal degree of coherence given by Eq. (12) for (a) $N = 2$ and (b) $N = 20$.

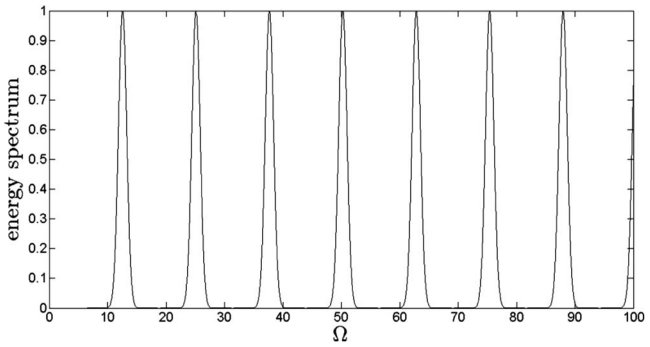

Fig. 2. Energy spectrum in arbitrary units for the case of $N = 20$ equally weighted modes with the period $a = 0.25$.

Here $X = x/\sigma_{\mathrm{I}}$, $Y = y/\sigma_{\mathrm{I}}$ are dimensionless Cartesian coordinates scaled to an arbitrary spatial scale in the transverse pane of the beam; all spatial scales are assumed to be normalized to σ_{I} henceforth. As it will become clear in the following, σ_{I} does in this case coincide with the rms width of the source intensity profile. By analogy with the temporal case, each factor in the cross-spectral density product (14) can be expressed in terms of pseudo-modes as

$$W(s_1, s_2) = \sum_{n_s} \nu_{n_s} \psi^*_{\alpha_{n_s}}(s_1) \psi_{\alpha_{n_s}}(s_2), \tag{15}$$

where

$$\psi_{\alpha_{n_s}}(s) = \frac{e^{-(\mathrm{Im}\,\alpha_{n_s})^2}}{\pi^{1/4}} \exp\left[-\frac{\left(s - \sqrt{2}\alpha_{n_s}\right)^2}{2}\right]. \tag{16}$$

It follows at once from the definition of the spectral degree of coherence [1,24] that

$$\mu(\boldsymbol{\rho}_1, \boldsymbol{\rho}_2) \equiv \frac{W(\boldsymbol{\rho}_1, \boldsymbol{\rho}_2)}{\sqrt{I(\boldsymbol{\rho}_1) I(\boldsymbol{\rho}_2)}}. \tag{17}$$

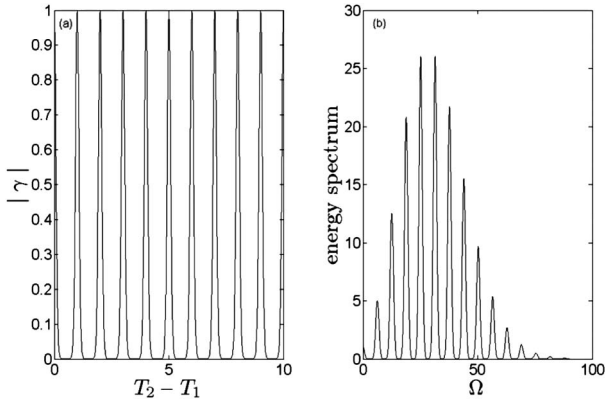

Fig. 3. Magnitude of the temporal degree of coherence (a) and the energy spectrum in arbitrary units (b) for the case when the modes are distributed according to $\nu_n = \lambda^n/n!$ with $\lambda = 5$ and $a = 0.25$.

Equations (15)–(17), and a 2D analog of (6) yield a Gaussian source intensity profile,

$$I(\boldsymbol{\rho}) \equiv W(\boldsymbol{\rho}, \boldsymbol{\rho}) \propto e^{-(X^2+Y^2)}, \tag{18}$$

justifying the identification of the scaling length with the rms source width, and the source coherence pattern in the form

$$\mu(\boldsymbol{\rho}_1, \boldsymbol{\rho}_2) = \prod_{s=X,Y} \frac{\sum_{n_s} \nu_{n_s} \exp\left[i \frac{\pi n_s}{a_s}(s_2 - s_1)\right]}{\sum_{n_s} \nu_{n_s}}. \tag{19}$$

In particular, the spectral degree of coherence magnitude of an optical lattice with $\nu_{n_s} = \nu = \mathrm{const}$, $0 \le n_s \le N$, can be written explicitly as

$$|\mu(\boldsymbol{\rho}_1, \boldsymbol{\rho}_2)| = \frac{1}{N^2} \left| \prod_{s=X,Y} \frac{\sin\left[\frac{\pi N}{2a_s}(s_2 - s_1)\right]}{\sin\left[\frac{\pi}{2a_s}(s_2 - s_1)\right]} \right|. \tag{20}$$

To illustrate the spectral degree of coherence behavior, we display in Fig. 4, $|\mu|$ for a spatial coherence lattice composed of $N = 20$ equally weighted Gaussian beams with the lattice aspect ratio $a_X/a_Y = 0.7$. The lattice-like coherence behavior is transparent from the figure.

The far-field angular distribution, generated by new sources, is specified by the radiant intensity J which can be expressed in the paraxial approximation as [1]

$$J(\mathbf{k}) = \int \mathrm{d}\boldsymbol{\rho}_1 \int \mathrm{d}\boldsymbol{\rho}_2 W(\boldsymbol{\rho}_1, \boldsymbol{\rho}_2) \exp[i\mathbf{k} \cdot (\boldsymbol{\rho}_1 - \boldsymbol{\rho}_2)], \tag{21}$$

where $\mathbf{k}$ is a 2D wave vector in the transverse plane of the source. Owning to a mathematical analogy between Eqs. (10) and (21), the radiant intensity distribution of a spatial coherence lattice can be expressed as

$$J(\mathbf{k}) \propto \prod_{s=X,Y} \sum_{n_s} \nu_{n_s} e^{-(K_s - \pi n_s/a_s)^2}, \tag{22}$$

where $K_{X,Y} = k_{x,y}\sigma_{\mathrm{I}}$. The radiant intensity is displayed in Fig. 5 in arbitrary units assuming the same weight distributions for the modes in the X and Y-directions, $\nu_{n_X} = \nu_{n_Y} = \lambda^{n_{X,Y}}/n_{X,Y}!$. For sufficiently small lattice constants $a_{X,Y}$ that we used, the angular distribution

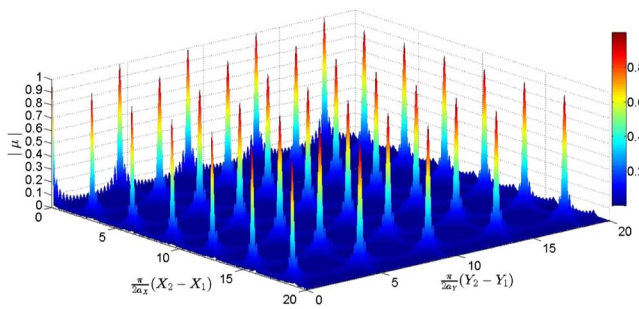

Fig. 4. Magnitude of the spectral degree of coherence for a spatial coherence lattice composed of $N = 20$ equally weighted modes; the aspect ratio of lattice constants, $a_X/a_Y = 0.7$.

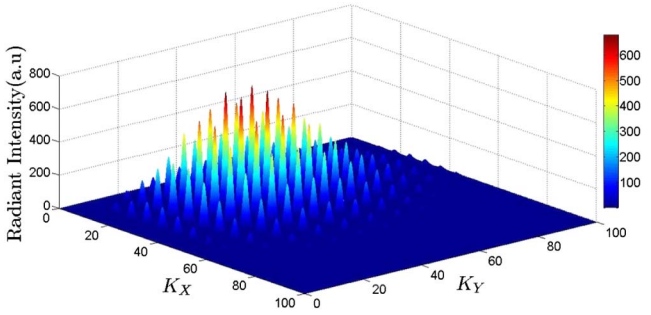

Fig. 5. Radiant intensity distribution of a spatial coherence lattice composed of $N = 20$ modes distributed according to $\nu_{n_{X,Y}} = \lambda^{n_{X,Y}}/n_{X,Y}!$ with $\lambda = 5$ and $a = 0.25$; the aspect ratio of lattice constants, $a_X/a_Y = 0.7$.

of the source radiation pattern is seen in the figure to be an amplitude-modulated periodic lattice of highly directional individual lobes.

In summary, we introduced novel classes of partially coherent Schell-model spatial and temporal sources. New temporal sources, temporal coherence gratings, have Gaussian intensity profiles and periodic coherence properties, yielding periodic energy spectra in the form of frequency combs. New spatial sources, spatial coherence lattices, also have Gaussian intensity profiles and lattice-like spectral degrees of coherence. The latter circumstance causes them to generate lattice-like radiation patterns composed of highly directional individual lobes. Temporal coherence gratings and induced frequency combs can find metrology and optical communications applications. Spatial coherence lattices can be used for material processing, robust (speckle-free) imaging with partially coherent light, and distortion-less information/image transfer through fluctuating natural environments such as the turbulent atmosphere.

References

1. L. Mandel and E. Wolf, *Optical Coherence and Quantum Optics* (Cambridge University, 1997).
2. R. Simon and N. Mukunda, J. Opt. Soc. Am. A **10**, 95 (1993).
3. R. Simon and N. Mukunda, J. Opt. Soc. Am. A **10**, 2008 (1993).
4. S. A. Ponomarenko, Phys. Rev. E **64**, 036618 (2001).
5. F. Gori, G. Guattari, and C. Padovani, Opt. Commun. **64**, 311 (1987).
6. S. A. Ponomarenko, J. Opt. Soc. Am. A **18**, 150 (2001).
7. S. A. Ponomarenko, W. Huang, and M. Cada, Opt. Lett. **32**, 2508 (2007).
8. A. T. Friberg, E. Tervonen, and J. Turunen, J. Opt. Soc. Am. A **11**, 1818 (1994).
9. G. V. Bogatyryova, C. V. Fel'de, P. V. Polyanskii, S. A. Ponomarenko, M. S. Soskin, and E. Wolf, Opt. Lett. **28**, 878 (2003).
10. F. Gori and M. Santarsiero, Opt. Lett. **32**, 3531 (2007).
11. H. Lajunen and T. Saastamoinen, Opt. Lett. **36**, 4104 (2011).
12. S. Sahin and O. Korotkova, Opt. Lett. **37**, 2970 (2012).
13. Z. Mei and O. Korotkova, Opt. Lett. **38**, 91 (2013).
14. Z. Mei and O. Korotkova, Opt. Lett. **38**, 2578 (2013).
15. L. Ding, O. Korotkova, Y. T. Zhang, and L. Z. Pan, Opt. Express **22**, 931 (2014).
16. O. Korotkova, Opt. Lett. **39**, 64 (2014).
17. L. Ding, O. Korotkova, and L. Z. Pan, Phys. Lett. A **378**, 1687 (2014).
18. M. Santarsiero, G. Piquero, J. C. G. de Sande, and F. Gori, Opt. Lett. **39**, 1713 (2014).
19. P. Vahimaa and J. Turinen, Opt. Express **14**, 1376 (2006).
20. S. A. Ponomarenko, Opt. Express **19**, 17086 (2011).
21. R. Martinez-Herrero, P. M. Mejias, and F. Gori, Opt. Lett. **34**, 1399 (2009).
22. S. A. Ponomarenko, G. P. Agrawal, and E. Wolf, Opt. Lett. **29**, 394 (2004).
23. J. W. Goodman, *Introduction to Fourier Optics*, 2nd ed. (McGraw-Hill, 1998).
24. S. A. Ponomarenko, H. Roychowdhury, and E. Wolf, Phys. Lett. A **345**, 10 (2005).